EBioMedicine 15 (2017) 36–47

Contents lists available at ScienceDirect

EBioMedicine

journal homepage: www.ebiomedicine.com

Research Paper

Enhanced Mucosal Defense and Reduced Tumor Burden in Mice with the Compromised Negative Regulator IRAK-M

Daniel E. Rothschild [a], Yao Zhang [b], Na Diao [b], Christina K. Lee [b], Keqiang Chen [b], Clayton C. Caswell [a], Daniel J. Slade [c], Richard F. Helm [c], Tanya LeRoith [a], Liwu Li [b,*], Irving C. Allen [a,**]

[a] Department of Biomedical Sciences and Pathobiology, VA-MD College of Veterinary Medicine, Blacksburg, Virginia 24061, United States
[b] Department of Biological Sciences, Virginia Polytechnic and State University, Blacksburg, Virginia 24061, United States
[c] Department of Biochemistry, Virginia Polytechnic and State University, Blacksburg, Virginia 24061, United States

ARTICLE INFO

Article history:
Received 11 August 2016
Received in revised form 30 November 2016
Accepted 30 November 2016
Available online 3 December 2016

Keywords:
Colitis
Colitis associated cancer
GALT
Inflammatory bowel disease
IRAK-M

ABSTRACT

Aberrant inflammation is a hallmark of inflammatory bowel disease (IBD) and colorectal cancer. IRAK-M is a critical negative regulator of TLR signaling and overzealous inflammation. Here we utilize data from human studies and *Irak-m*$^{-/-}$ mice to elucidate the role of IRAK-M in the modulation of gastrointestinal immune system homeostasis. In human patients, *IRAK-M* expression is up-regulated during IBD and colorectal cancer. Further functional studies in mice revealed that *Irak-m*$^{-/-}$ animals are protected against colitis and colitis associated tumorigenesis. Mechanistically, our data revealed that the gastrointestinal immune system of *Irak-m*$^{-/-}$ mice is highly efficient at eliminating microbial translocation following epithelial barrier damage. This attenuation of pathogenesis is associated with expanded areas of gastrointestinal associated lymphoid tissue (GALT), increased neutrophil migration, and enhanced T-cell recruitment. Further evaluation of *Irak-m*$^{-/-}$ mice revealed a splice variant that robustly activates NF-κB signaling. Together, these data identify IRAK-M as a potential target for future therapeutic intervention.

1. Introduction

Crohn's disease (CD) and ulcerative colitis (UC) represent the clinical manifestations of inflammatory bowel disease (IBD). In humans, there is a strong association in patients afflicted with IBD to further develop colitis associated cancer (CAC) (Greten et al., 2004). Gastrointestinal (GI) immune homeostasis is, in part, maintained by pattern recognition receptors (PRRs); including, but not limited to the Toll-like receptors (TLRs). There are 10 known TLRs in humans that recognize pathogen associated molecular patterns (PAMPs) associated with invading microbes (Kawai and Akira, 2011). In the gut, TLRs sense and respond to commensal flora translocation, resulting from damage to the epithelial cell barrier during the course of disease progression (Saleh and Elson, 2011). Following TLR engagement to its pathogenic ligand, a highly coordinated signaling cascade leads to the activation of specific transcription factors including nuclear factor-κB (NF-κB), activating protein-1 (AP-1), or in the case of viral recognition, interferon regulatory factor-3 (IRF-3). The signaling pathway utilized depends upon which TLR is stimulated in response to the pathogenic ligand; however, all TLRs, with the exception of TLR-3, signal through the myeloid differentiation factor 88 (MyD88) adaptor molecule (Kawai et al., 1999; Takeuchi et al., 2000; Jiang et al., 2006). A MyD88 independent pathway exists for both TLR-3 and TLR-4 that has been shown to signal through the adaptor molecule TIR-domain-containing-adapter-inducing interferon-β (TRIF) (Yamamoto et al., 2003; Hoebe et al., 2003; Kawai et al., 2001). In healthy individuals, these TLR signaling cascades are responsible for rapid activation of innate host defenses and further activation of the adaptive immune response (Medzhitov and Janeway, 1997). However, uncontrolled activation of TLR signaling promotes chronic inflammation and is associated with a variety of autoimmune diseases, including IBD (Cook et al., 2004).

The TLRs that utilize the MyD88 dependent pathway have been reported to signal through a family of Interleukin Receptor Associated Kinases (IRAKs), which contain four known family members being: IRAK-1, IRAK-2, IRAK-M, and IRAK-4 (Wesche et al., 1997; Muzio et al., 1997; Wesche et al., 1999; Li et al., 2002). IRAK-1, IRAK-2, and IRAK-4 have been described to play a role in the transduction of downstream signaling from MyD88; conversely, IRAK-M is rather unique and has been shown to be a negative regulator of TLR signaling (Kobayashi et al., 2002). The initial reports pertaining to IRAK-M described it as a member of the Pelle/IRAK family, and when overexpressed in mammalian cells,

* Correspondence to: L. Li, 970 Washington Street, Life Science 1 Building, Department of Biological Sciences, Virginia Tech, Blacksburg, VA 24061-0910, United States.
** Correspondence to: I. C. Allen, Department of Biomedical Sciences and Pathobiology, Virginia-Maryland College of Veterinary Medicine, Virginia Tech, 295 Duckpond Drive, Blacksburg, VA 24061, United States.
E-mail addresses: lwli@vt.edu (L. Li), icallen@vt.edu (I.C. Allen).

http://dx.doi.org/10.1016/j.ebiom.2016.11.039

had the capacity to activate NF-κB through interactions with TNF receptor associated factor-6 (TRAF-6) (Wesche et al., 1999). Following the generation of an *Irak-m*$^{-/-}$ mouse, IRAK-M was confirmed to function as a negative regulator of TLR signaling (Kobayashi et al., 2002).

Here we report that *IRAK-M* is significantly up-regulated in human patients with IBD and colitis associated neoplasia. We also show that *IRAK-M* is up-regulated in advanced stages of colorectal cancer (CRC). Prior studies have evaluated IRAK-M in models of experimental colitis and colitis associated tumorigenesis utilizing *Irak-m*$^{-/-}$ mice and shown that these animals are highly sensitive to both inflammation and neoplasia. However, contrary to these prior observations, more recent studies have revealed that *Irak-m*$^{-/-}$ mice are actually protected from inflammation driven tumorigenesis in the colon (Kesselring et al., 2016). IRAK-M was found to support colorectal cancer progression through the reduction of antimicrobial defenses and the stabilization of STAT-3 (Kesselring et al., 2016). Due to these conflicting reports, we sought to better elucidate the contribution of IRAK-M during IBD and colitis associated tumorigenesis. Our studies are, in general, complementary to the more recent findings that support a role for IRAK-M in disease pathogenesis. Here we report that *Irak-m*$^{-/-}$ mice were significantly protected against dextran sulfate sodium (DSS)-mediated GI inflammation and azoxymethane (AOM)/DSS mediated tumor formation. We further show that the immune system in the GI tract of *Irak-m*$^{-/-}$ mice is primed and highly efficient at eliminating components of the microbiome translocating from the GI lumen following damage to the epithelial barrier. This priming and attenuation of disease appears to be associated with expanded areas of gastrointestinal associated lymphoid tissue (GALT), increased and efficient neutrophil migration, and enhanced T-cell recruitment.

Upon further evaluation of the *Irak-m*$^{-/-}$ mice, we discovered the formation of a *Irak-m* splice variant. The splicing event joins exon 8 with exon 12, splicing around the neomycin resistance cassette (Kobayashi et al., 2002), forming a *Irak-m*$^{r\Delta 9-11}$ truncation mutant. This truncation mutant functions to robustly induce NF-κB signaling when overexpressed in HEK293T cells. Together, our data confirms previous findings that IRAK-M functions as a critical mediator of inflammatory signaling pathways and is essential to maintaining immune system homeostasis in the GI system.

2. Materials and Methods

2.1. Human Metadata Analysis

IRAK-M expression was assessed using a publicly accessible microarray metadata analysis search engine (http://www.nextbio.com/b/nextbioCorp.nb), as previously described (Kupershmidt et al., 2010). The following array data series were analyzed to generate the human patient and cell expression data: GSE10714; GSE59071; GSE9686; GSE13367; GSE36807; GSE16879; GSE10191; GSE52746; GSE9452; GSE38713; GSE4183; GSE37283; GSE37364; GSE10715.

2.2. Experimental Animals

All mouse studies were approved by the Institute for Animal Care and Use Committee (IACUC) at Virginia Tech and in accordance with the Federal NIH *Guide for the Care and Use of Laboratory Animals*. The *Irak-m*$^{-/-}$ mice were generated as previously described (Kobayashi et al., 2002) and purchased from The Jackson Laboratory. All studies were controlled with either littermate and/or co-housed WT animals that were maintained under specific pathogen-free conditions and received standard chow (LabDiet) and water *ad libitum*. All experiments described utilized age matched male mice.

2.3. Experimental Colitis and Colitis Associated Tumorigenesis

In order to assess acute experimental colitis, mice were given either 3 or 5% DSS dissolved in drinking water available *ad libitum* for 5 days as previously described (Williams et al., 2015b; Schneider, 2013). On day 5, mice were withdrawn from DSS and given regular drinking water *ad libitum* until euthanasia was performed on day 7. Cumulative semi quantitative clinical scores for acute experimental colitis were assessed as previously described (Williams et al., 2015b; Schneider, 2013). Tumorigenesis was induced *via* a single intraperitoneal (i.p.) injection of AOM (10 mg/kg of total body weight) and supplemented with three cycles of 2.5% DSS in drinking water available *ad libitum* for 5 days with 2 weeks of recovery between cycles, as previously described (Neufert et al., 2007; Allen et al., 2010). While subjected to DSS, mice were monitored for weight loss, physical body condition, stool consistency, and rectal bleeding. Upon completion of each model, whole blood was collected by cardiac puncture for bacterial counts, flow cytometry assessments of leukocyte populations, and serum isolation. Colon sections were collected for H&E staining. Blinded to treatment and mouse genotype, examination of histopathology was conducted by a board-certified veterinary pathologist (T.L.). Colon H&E sections were evaluated and scored as previously described (Williams et al., 2015b). Additional colon sections were further prepared for immunohistochemistry and stained with *anti*-β-catenin and DAPI to determine β-catenin levels in the AOM + DSS studies.

2.4. FACS

Leukocytes and lymphocytes were evaluated from either: bone marrow, spleen, or whole blood utilizing flow cytometry. Cells were immunostained with antibodies for the respective cell surface markers prior to FACS analysis. Sorted cells were further evaluated for CXCR2, CD14, CD11b+, Ly6G+, CD4+, CD8+, Ly6C+, IAE, and CD62L.

2.5. ELISA

Cell culture supernatants or colon organ culture supernatants were collected from each individual well in 1.7 ml tubes and centrifuged at 300 × *g* for 10 min to remove residual cells. Cell-free supernatants were then assayed for mouse IL-6 and/or IL-10 (BD Biosciences) according to the manufacturer's instructions.

2.6. Statistical Analysis

Data are represented as mean ± standard error of mean (S.E.M.) unless otherwise indicated. Graphs and statistical analysis were conducted *via* GraphPad PRISM software. Complex data sets were analyzed by 1 way analysis of variance (ANOVA) and followed by either Tukey-Kramer HSD or Newman-Keuls method. The Kaplan-Meier test was conducted to determine group survival. A value of $p < 0.05$ was considered statistically significant.

3. Results

3.1. IRAK-M Expression Is significantly Increased in Human Patients with IBD and CRC

Previous studies have shown that *IRAK-M* expression is increased in IBD patients (Fernandes et al., 2016; Gunaltay et al., 2014). Thus, we initially sought to evaluate these findings and expand our analysis to further evaluate *IRAK-M* expression in the context of colitis associated neoplasia and CRC using a retrospective metadata analysis of publicly available gene expression data (Kupershmidt et al., 2010). Our analysis revealed that the relative expression of *IRAK-M* is significantly increased in human patients with active forms of IBD (Fig. 1A). Patients that suffer from IBD have a higher predisposition to CAC (Karlen et al., 1999); thus,

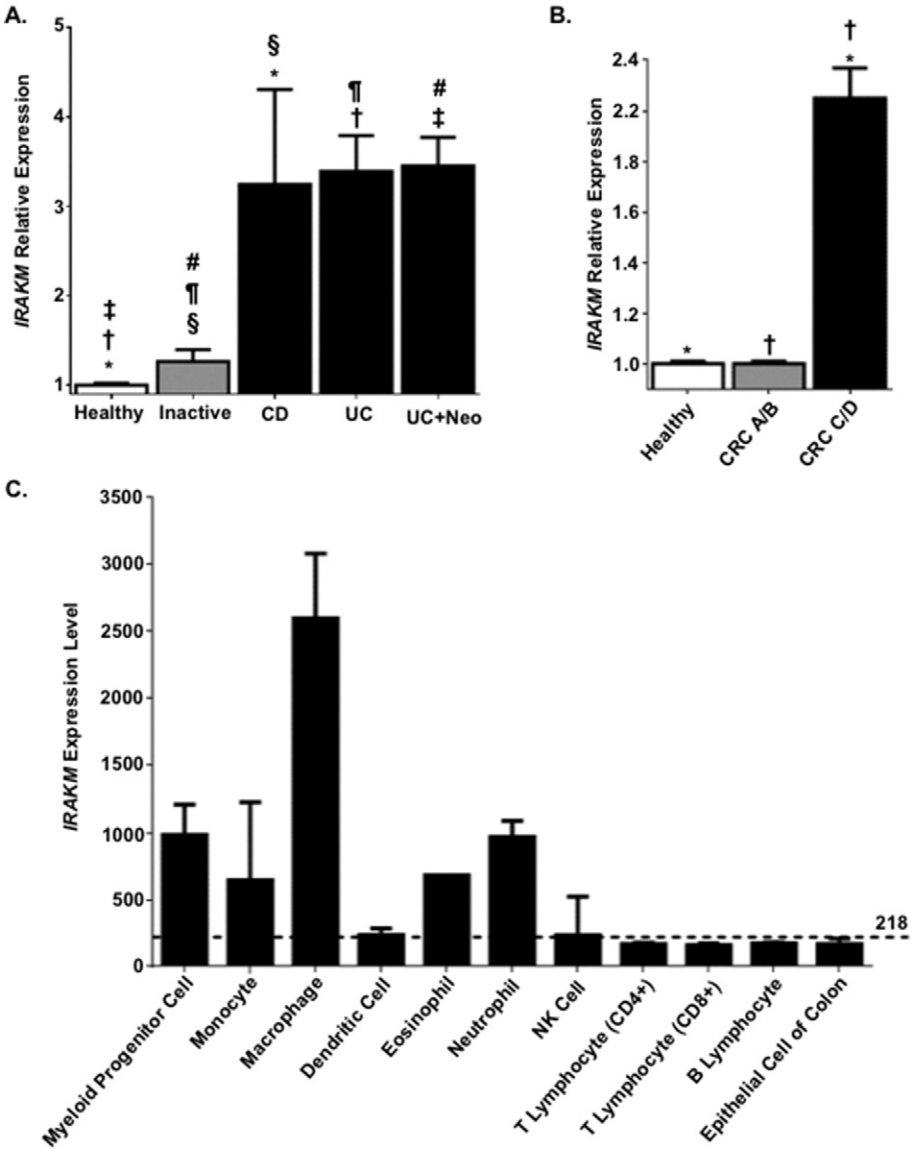

Fig. 1. *IRAK-M* expression is increased during inflammatory bowel disease exacerbation and in advanced colorectal cancer patients. A. Retrospective analysis of metadata from colonic biopsies revealed that *IRAK-M* expression was significantly increased in Crohn's disease (CD) and ulcerative colitis (UC) patients during exacerbation, compared to biopsies from currently diagnosed IBD patients during inactive disease (inactive) and patients not diagnosed with IBD (healthy). *IRAK-M* was also significantly up-regulated in UC patients with neoplasia (UC + Neo). The fold-change values were extracted and averaged from 7 separate datasets and reflect the change in *IRAK-M* expression between each patient population and the respective healthy controls. *, †, ‡, §, ¶, #$p < 0.05$. B. Colorectal cancer (CRC) patients were stratified based on the Dukes' staging system (A/B) and (C/D). *IRAK-M* expression was significantly increased in patients with more advanced disease (CRC C/D) compared to the less advanced (CRC A/B) patients and patients not diagnosed with CRC (healthy). The fold-change values were extracted and averaged from 2 separate datasets and reflect the change in *IRAK-M* expression between each patient population and the respective healthy controls. *, † $p < 0.05$. **C.** *IRAK-M* is differentially expressed in multiple human cell types of relevance to IBD and CRC, with the highest levels of expression in cells of the myeloid lineage. The mean expression of *IRAK-M* in all human cell types is identified by the dotted line (218).

we also included CAC patients in our data analysis and found that *IRAK-M* is also significantly increased in patients with active UC with inclusive areas of neoplasia (Fig. 1A). Independent of CAC, we were also interested in evaluating *IRAK-M* expression in the context of CRC. Thus, we also analyzed expression levels of *IRAK-M* in patients diagnosed with both low and high-grade CRC. CRC patients were stratified based on the Dukes' staging system (A/B) and (C/D). From these data, it is apparent that *IRAK-M* expression is significantly increased in patients with more advanced CRC (grades C/D) compared to the patients with less advanced CRC (grades A/B) and patients not diagnosed with CRC (Fig. 1B). To gain greater insight into *IRAK-M* function, we next sought to evaluate *IRAK-M* expression in different human cell types of relevance to IBD, CAC, and CRC, with particular emphasis on specific immune cell populations and colon epithelial cells (Fig. 1C). Prior literature documents the expression of *IRAK-M* in cells of the myeloid linage (Wesche et al., 1999). This is supported by our metadata analysis (Fig. 1C). However, our findings further revealed that *IRAK-M* is also highly expressed in eosinophils and neutrophils (Fig. 1C). We also found *IRAK-M* expressed in all of the other cell types assessed, albeit at lower levels than the macrophages, myeloid progenitor cells and granulocytes (Fig. 1C). Together, these data suggest that IRAK-M plays a significant role in modulating the immune response in the GI system and is up-regulated in the context of IBD and CRC. This up-regulation is likely in response to increased TLR and interleukin 1 receptor (IL-1R1) signaling in these disease states.

3.2. Irak-m$^{-/-}$ Mice Are Protected against DSS Induced Colitis

We next sought to better characterize the contribution of IRAK-M in the context of IBD. Prior studies have evaluated *Irak-m*$^{-/-}$ mice in both dextran sulfate sodium (DSS) and *Il10*$^{-/-}$ colitis models (Berglund et al.,

2010; Biswas et al., 2011). These prior studies revealed that IRAK-M functions to attenuate the progression of experimental colitis (Berglund et al., 2010; Biswas et al., 2011). Here we utilized *Irak-m*$^{-/-}$ mice in an acute colitis model induced with 5% DSS (Okayasu et al., 1990). This is a standard model utilized previously by our laboratory in similar studies evaluating mediators of innate immunity in IBD (Williams et al., 2015a, 2015b; Allen et al., 2012, 2010). We found that *Irak-m*$^{-/-}$ mice are protected in this experimental colitis model (Fig. 2). Clinically, the *Irak-m*$^{-/-}$ mice demonstrate significant improvements in weight change and clinical parameters associated with disease progression compared to the wild-type (WT) animals (Fig. 2A and B). Consistent with our clinical observations, *Irak-m*$^{-/-}$ mice also displayed significantly increased colon length and less severe tissue damage as evident by histopathology evaluation of H&E stained colon sections compared to the WT counterparts (Fig. 2C and D). Interestingly, when viewing the histopathology of the colon from *Irak-m*$^{-/-}$ mice we observed localized and highly structured areas of lymphoid cells throughout the colon. These structures were identified and confirmed to be expanded areas gut associated lymphoid tissue (GALT) by a board certified veterinary pathologist (T.L.) (Fig. 2E). We hypothesized that the protective phenotype observed in the *Irak-m*$^{-/-}$ mice following acute DSS exposure was due, in part, to the significant increase in GALT in the colon of the *Irak-m*$^{-/-}$ mice, which were present irrespective of DSS treatment (Fig. 2E). To test this hypothesis, we measured the systemic bacteremia in whole blood of both WT and *Irak-m*$^{-/-}$ mice following the acute DSS model. Our data lend support to this hypothesis as bacterial counts were significantly reduced in *Irak-m*$^{-/-}$ mice (Fig. 2F). Further, we observed increased levels of IL-6 from *Irak-m*$^{-/-}$ colon organ culture supernatant following DSS treatment, which is consistent with the increased GALT (Fig. 2G). While increased IL-6 is typically associated with detrimental inflammation, our histopathology assessments revealed that the inflammation was highly localized to these areas of GALT, with minimal damage to the epithelial cell barrier (Fig. 2D). Collectively, our data suggest that *Irak-m*$^{-/-}$ mice are protected against DSS induced colitis by displaying increased resistance to bacterial translocation and bacteremia.

3.3. Attenuation of Experimental Colitis in the *Irak-m*$^{-/-}$ Mice Is Associated with Enhanced Neutrophil and T-Cell Responses

We hypothesized that the increased GALT observed in the *Irak-m*$^{-/-}$ mice was a significant contributing factor in protecting these animals during experimental colitis. To test whether *Irak-m*$^{-/-}$ protection from acute DSS was associated with increased leukocyte recruitment and function, we evaluated the leukocyte composition in whole blood using flow cytometry (Fig. 3A). Under basal conditions, we found the neutrophil count was significantly higher in the blood from naïve *Irak-m*$^{-/-}$ mice compared to WT animals (Fig. 3A). Interestingly, following exposure to DSS the number of neutrophils significantly increased in WT mice; however, the number of neutrophils in the *Irak-m*$^{-/-}$ mice maintained elevated levels with or without exposure to DSS (Fig. 3A). We further measured the levels of CXCR2 and CD14 from both naïve animals and mice in the experimental colitis model (Fig. 3B and C). Under both naïve and DSS treated conditions, we observed increased levels of CXCR2 and CD14 from *Irak-m*$^{-/-}$ Ly6G^{+}/CD11b^{+} leukocytes, suggesting *Irak-m*$^{-/-}$ neutrophils are primed prior to tissue insult, which likely improves the efficiency in recruitment to a site of infection, such as the colon when bacterial translocation occurs. To further support this hypothesis, we performed a neutrophil chemotaxis assay in response to macrophage inflammatory protein 2 (MIP-2). When bone marrow from WT and *Irak-m*$^{-/-}$ mice was primed with doses of LPS and subjected to the chemotaxis assay, we observed increases in neutrophils in a dose dependent manner for *Irak-m*$^{-/-}$ mice (Fig. 3D). Further, we also observed increased numbers of CD4^{+}, CD8^{+} T-cells and monocytes isolated from the spleen of *Irak-m*$^{-/-}$ mice following exposure to DSS (Fig. 3E). This finding is consistent with prior studies that indicated increased T-cell recruitment in *Irak-m*$^{-/-}$ mice in the experimental colitis model (Berglund et al., 2010; Klimesova et al., 2013). Monocytes isolated from the spleen of *Irak-m*$^{-/-}$ mice following DSS exposure displayed increased cell surface expression of IAE and decreased expression of CD62L (Fig. 3F). Further, we hypothesized that the differences in neutrophil and T-cell recruitment in *Irak-m*$^{-/-}$ mice was the result of differences associated with the GI microbiota composition. When mice were treated with antibiotics for two weeks prior to DSS administration, similar susceptibilities to pathogenesis were observed between WT and *Irak-m*$^{-/-}$ mice (Fig. S1A—C). Collectively, our data suggests that *Irak-m*$^{-/-}$ mice are protected from experimental colitis due to efficient recruitment of neutrophils and T-cells following microbial translocation. These data provide a mechanism of acute colitis protection and lend support to the phenotype that GALT in *Irak-m*$^{-/-}$ mice contributes to the overall protection observed in the experimental colitis model.

3.4. *Irak-m*$^{-/-}$ Mice Are Protected against Inflammation Driven Colon Tumorigenesis

Our retrospective metadata analysis revealed that IRAK-M likely modulates IBD, CAC, and CRC in human patients (Fig. 1A and B). Based on our findings in the IBD model, we next sought to evaluate the *Irak-m*$^{-/-}$ mice in a model of colitis associated tumorigenesis. Here we utilized the AOM + DSS model (Williams et al., 2015a; Allen et al., 2012, 2010). *Irak-m*$^{-/-}$ mice displayed improved morbidity and mortality throughout the course of the model compared to the WT animals, suggesting attenuation of disease progression compared to the WT counterparts (Fig. 4A-C). When colon organ culture supernatants were assayed for IL-6 and IL-10, *Irak-m*$^{-/-}$ mice displayed significant increases in both cytokines (Fig. 4D–E). Beyond the significant attenuation of clinical features and enhanced cytokine responses, the *Irak-m*$^{-/-}$ mice displayed dramatic resistance to tumorigenesis (Fig. 5). The overall gross polyp formation was significantly higher in WT mice; conversely, no polyps were detected in *Irak-m*$^{-/-}$ mice over the course of the study (Fig. 5A–C). Decreased tumor burden was further supported by histopathology assessments of H&E stained colon sections (Fig. 5D). As described for the experimental colitis model, GALT formation was prominent in *Irak-m*$^{-/-}$ mice (Fig. 5E). Consistent with the macroscopic colon evaluation, histopathology scoring revealed significant reductions in areas of hyperplasia and dysplasia in *Irak-m*$^{-/-}$ mice (Fig. 5F and G). Likewise, we found that the levels of β-catenin are also markedly reduced in *Irak-m*$^{-/-}$ mice following AOM + DSS (Fig. 5H). Collectively, our data indicates that the *Irak-m*$^{-/-}$ mice are resistant to both experimental colitis and inflammation driven tumorigenesis.

3.5. Identification of a Splice Variant of the Irak-m Gene in *Irak-m*$^{-/-}$ Mice

Expression levels of *IRAK-M* are highest in macrophages and previous studies have utilized both human and mouse macrophages to study IRAK-M function (Wesche et al., 1999; Kobayashi et al., 2002). Thus, we were interested in determining the response of IRAK-M in murine bone marrow derived macrophages (BMDM) when challenged with diverse PAMPs. In our hands, BMDM from our *Irak-m*$^{-/-}$ mice display significantly increased levels of IL-6 compared to WT BMDMs when stimulated for 24 h with different TLR ligands, specifically the TLR1/2 ligand Pam3CSK4 (Fig. 6A). Further, we assessed a broad panel of secreted cytokines following 24 h treatment with TLR 1–9 agonists. Specifically, *Irak-m*$^{-/-}$ BMDMs display increased levels of TNF with TLR1/2 agonists and decreased IL-10 with TLR 1/2, 7, and 9 agonists (Fig. S2A–E). This is consistent with prior reports pertaining to IRAK-M being a negative regulator of TLR signaling (Kobayashi et al., 2002). We also observed differences in IL-6 secretion between male and female *Irak-m*$^{-/-}$ BMDMs when stimulated with Pam3CSK4 (Fig. S3). However, during routine follow-up studies, we observed IRAK-M protein induction in both the WT and *Irak-m*$^{-/-}$ strains when stimulated with

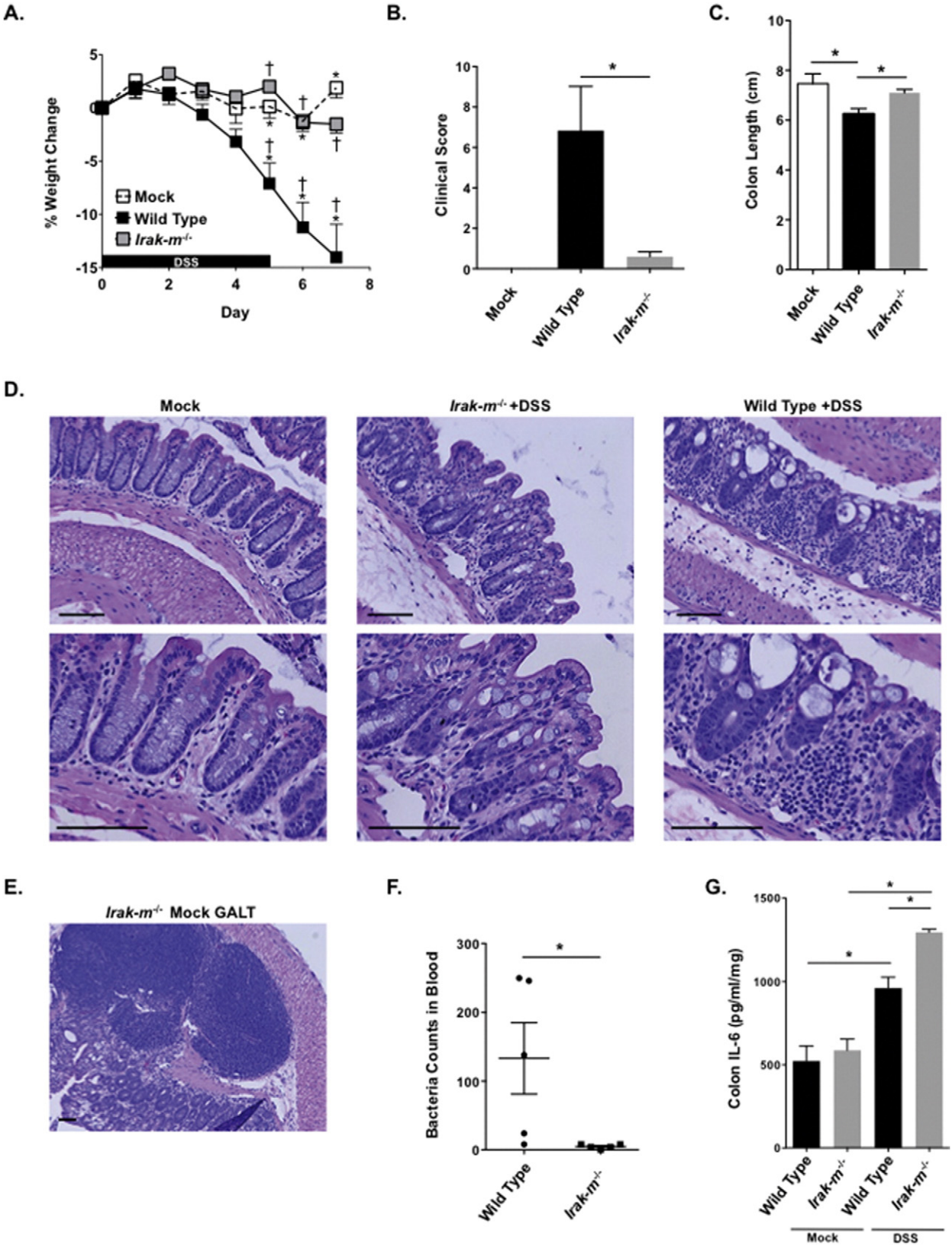

Fig. 2. Attenuated experimental colitis pathogenesis in *Irak-m*$^{-/-}$ Mice. A. *Irak-m*$^{-/-}$ mice demonstrated significantly improved weight change following DSS exposure compared to similarly treated WT mice. *Irak-m*$^{-/-}$ mock weight is not included for simplicity. B. Clinical features associated with disease progression were significantly attenuated in *Irak-m*$^{-/-}$ mice. C. *Irak-m*$^{-/-}$ mice had significantly increased colon length compared to WT animals. D. Representative H&E stained histopathology images of colon sections from WT and *Irak-m*$^{-/-}$ mice following the acute colitis model. Scale bars = 100 μm E. *Irak-m*$^{-/-}$ mice displayed large areas of Gut Associated Lymphoid Tissue (GALT), regardless of exposure to DSS. Scale bars = 100 μm. F. Bacteria count in 25 μl of blood from WT ($n = 5$) and *Irak-m*$^{-/-}$ mice ($n = 5$) with DSS induced colitis. G. IL-6 levels were significantly increased in colon sections harvested from *Irak-m*$^{-/-}$ mice following DSS exposure. Data are represented as mean ± SEM. $^{*}p < 0.05$; $^{\dagger}p < 0.05$ by 1 way ANOVA, Newman-Keuls post-test. WT mock, $n = 3$; WT DSS, $n = 6$; *Irak-m*$^{-/-}$ mock, $n = 3$ (not shown); *Irak-m*$^{-/-}$ DSS, $n = 5$. Data are representative of 3 independent studies.

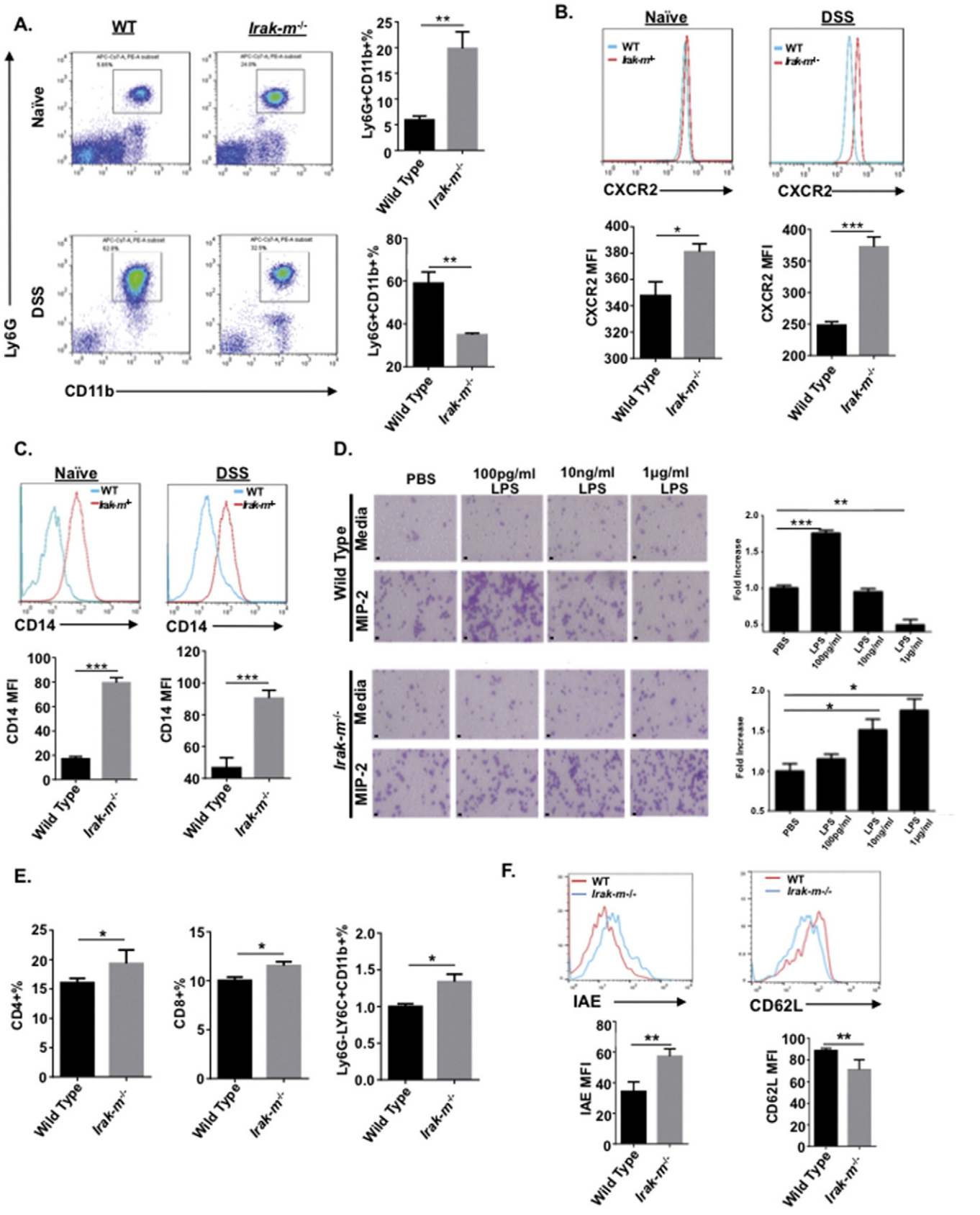

Fig. 3. Increased neutrophil and t-cell function in *Irak-m*$^{-/-}$ Mice. A. Representative FACS plots of neutrophils and the percentage of neutrophils (Ly6G + CD11b+) in the blood of naïve mice and mice with DSS-induced ulcerative colitis. B. The expression of CXCR2 on the Ly6G + CD11b + cells in the blood. C. The expression of CD14 on the Ly6G + CD11b + cells in the blood. $^{*}p < 0.05$, $^{**}p < 0.01$, $^{***}p < 0.001$, $n = 5$. D. Chemotaxis of neutrophils to MIP-2. Neutrophils purified from the bone marrow were primed with different doses of LPS, then subjected to chemotaxis assay. PBS is used as control. $^{*}p < 0.05$, $^{**}p < 0.01$, $^{***}p < 0.001$, $n = 5$. Scale bars = 10 μm. E. Percentages of CD4+, CD8 + T cells and monocytes in the spleen from mice with DSS-induced ulcerative colitis. F. The expression of IAE and CD62L on Ly6G-Ly6C + CD11b + monocytes in the spleen from mice with DSS-induced ulcerative colitis. $^{*}p < 0.05$, $^{**}p < 0.01$, $n = 4$.

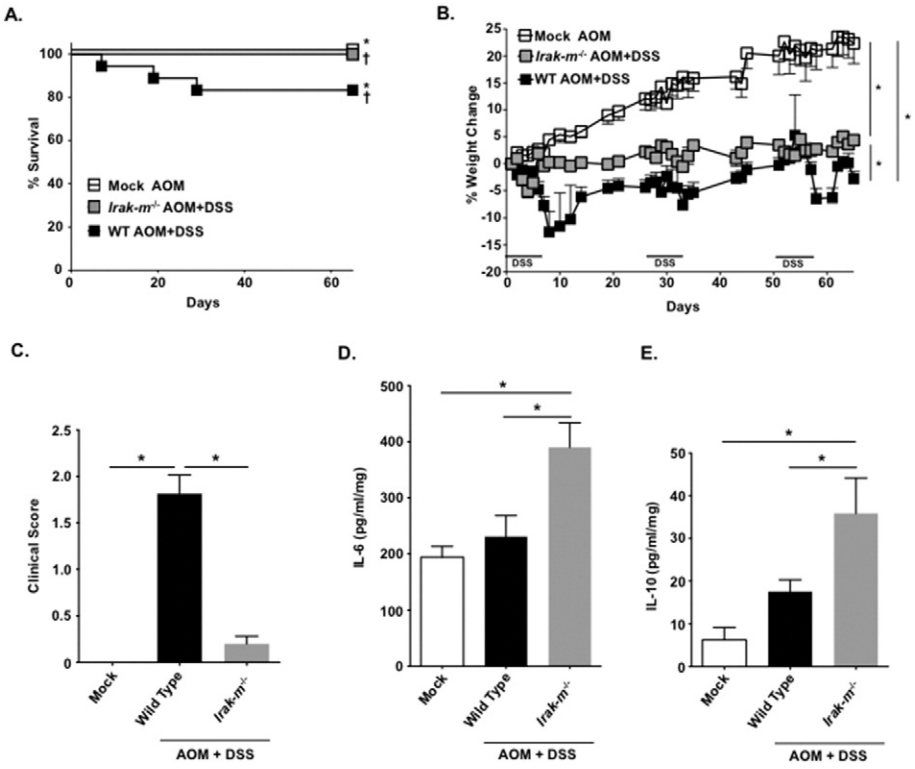

Fig. 4. Colitis associated tumorigenesis progression is significantly reduced in *Irak-m*$^{-/-}$ mice. A. Kaplan-Meier plot of *Irak-m*$^{-/-}$ and WT survival. $^{*}p < 0.05$; $^{\dagger}p < 0.05$. B. WT mice demonstrated significant weight loss throughout the AOM/DSS model, whereas weight loss in the *Irak-m*$^{-/-}$ mice was minimal. All mock and mock + AOM mice gained weight throughout the duration of the model, regardless of genotype. The WT mock + AOM are shown for comparison. C. Clinical features associated with disease progression were significantly improved in *Irak-m*$^{-/-}$ mice. Data shown reflect the clinical scores on the final day of the model (Day 65). D–E. Both IL-6 and IL-10 levels were significantly increased in colons harvested from *Irak-m*$^{-/-}$ mice compared to mock, mock + AOM, and WT AOM + DSS treated mice. Data are represented as mean ± SEM. $^{*}p < 0.05$; $^{\dagger}p < 0.05$; $p < 0.05$ by 1 way ANOVA, Newman-Keuls post-test. Mock WT, $n = 5$ (not shown); mock *Irak-m*$^{-/-}$, $n = 5$ (not shown); AOM + mock WT, $n = 5$; AOM + mock *Irak-m*$^{-/-}$, $n = 5$ (not shown); AOM + DSS WT, $n = 18$; AOM + DSS *Irak-m*$^{-/-}$, $n = 5$. Data are representative of 3 independent studies.

various TLR ligands using an antibody specific for the C-terminus of IRAK-M (Fig. S4). This was unexpected, as our *Irak-m*$^{-/-}$ mice were acquired from a commercial vendor, albeit reconstituted from frozen embryos, and previously characterized (Kobayashi et al., 2002). It was previously reported that generation of the *Irak-m*$^{-/-}$ mouse targeted exons 9–11 for deletion by homologous recombination inserting the neomycin resistance cassette in place of these three exons (Kobayashi et al., 2002). In order to test the hypothesis that IRAK-M was present in our mutant mice, we proceeded by further investigating the phenomena at the mRNA level. When BMDMs were stimulated for 24 h with the TLR1/2 ligand Pam3CSK4 to induce *Irak-m* transcription, we observed an amplification band corresponding specifically to exon 12 of *Irak-m* by RT-PCR (Fig. 6B). PCR primers were further designed to amplify the region spanning the length of exons 5 and 12 (Fig. 6C). Interestingly, a shift of approximately 400 bp was observed in the BMDMs from our *Irak-m*$^{-/-}$ animals, which suggested a splice variant had been generated. This was indeed confirmed by Sanger sequencing, which revealed a splice occurred after exon 8 and connecting it with exon 12 in the amplification band (Fig. 6D). Loss of the neo cassette only occurred at the mRNA level, likely after exon splicing, and not at the DNA level. This is evident because the genotyping primers are targeted against a portion of the neo cassette, which is present in the genotyping for the *Irak-m*$^{-/-}$ mice. Based on this revelation, we have defined this splice variant as *Irak-m*$^{r\Delta 9-11}$. In order to test the functionality of this truncated transcript, we cloned both the WT and mutant *Irak-m*$^{r\Delta 9-11}$ transcripts. Overexpression in HEK293T cells of both the WT and truncated *Irak-m*$^{r\Delta 9-11}$ transcripts both had the capacity to activate an NF-κB dependent luciferase reporter. However, NF-κB activation was robustly increased following overexpression of *Irak-m*$^{r\Delta 9-11}$ compared to the WT (Fig. 6E), suggesting a functional and potent role for this mutant protein. We further validated the specificity of the commercially available IRAK-M antibody used in Fig. S1, which displayed no specificity for the WT-IRAK-M or *Irak-m*$^{r\Delta 9-11}$ overexpression constructs (data not shown).

4. Discussion

Overzealous inflammation associated with dysregulated innate immune signaling is a significant component of IBD pathogenesis. This hyper-inflammation is often associated with aberrant TLR signaling. There is significant interest in better characterizing the contribution of proteins, like IRAK-M, that regulate PRR signaling in IBD, CAC, and CRC. This interest is due to the revelation that these regulatory proteins significantly attenuate disease pathogenesis in IBD mouse models. For example, prior studies by our group and others have shown that a diverse group of negative regulatory proteins, including NLRP12, NLRX1, TOLLIP, A20, and GIT2, also function to maintain immune system homeostasis in the gut through the attenuation of hyper-responsive inflammation (Mukherjee and Biswas, 2014; Vereecke et al., 2014; Hammer et al., 2011; Boj et al., 2015; Allen et al., 2012; Zaki et al., 2011; Soares et al., 2014; Singh et al., 2015). Many of these negative regulatory proteins have been found dysregulated in IBD and CRC patients. For example, previous reports have indicated that *IRAK-M* expression is significantly increased in IBD patients with both UC and CD (Fernandes et al., 2016; Gunaltay et al., 2014). These findings are consistent with our analysis of retrospective metadata that revealed increased *IRAK-M* expression, not only in active UC and CD patients, but also in the context of colitis associated neoplasia (Fig. 1). Our retrospective metadata analysis revealed that *IRAK-M* expression increases with severity of CRC progression (Fig. 1). Together these data likely reflect an increase in the innate immune response during both IBD and CRC that is driven by PRR activation. These data are consistent with recent findings that revealed increased IRAK-M induction in colon tumor cells associated

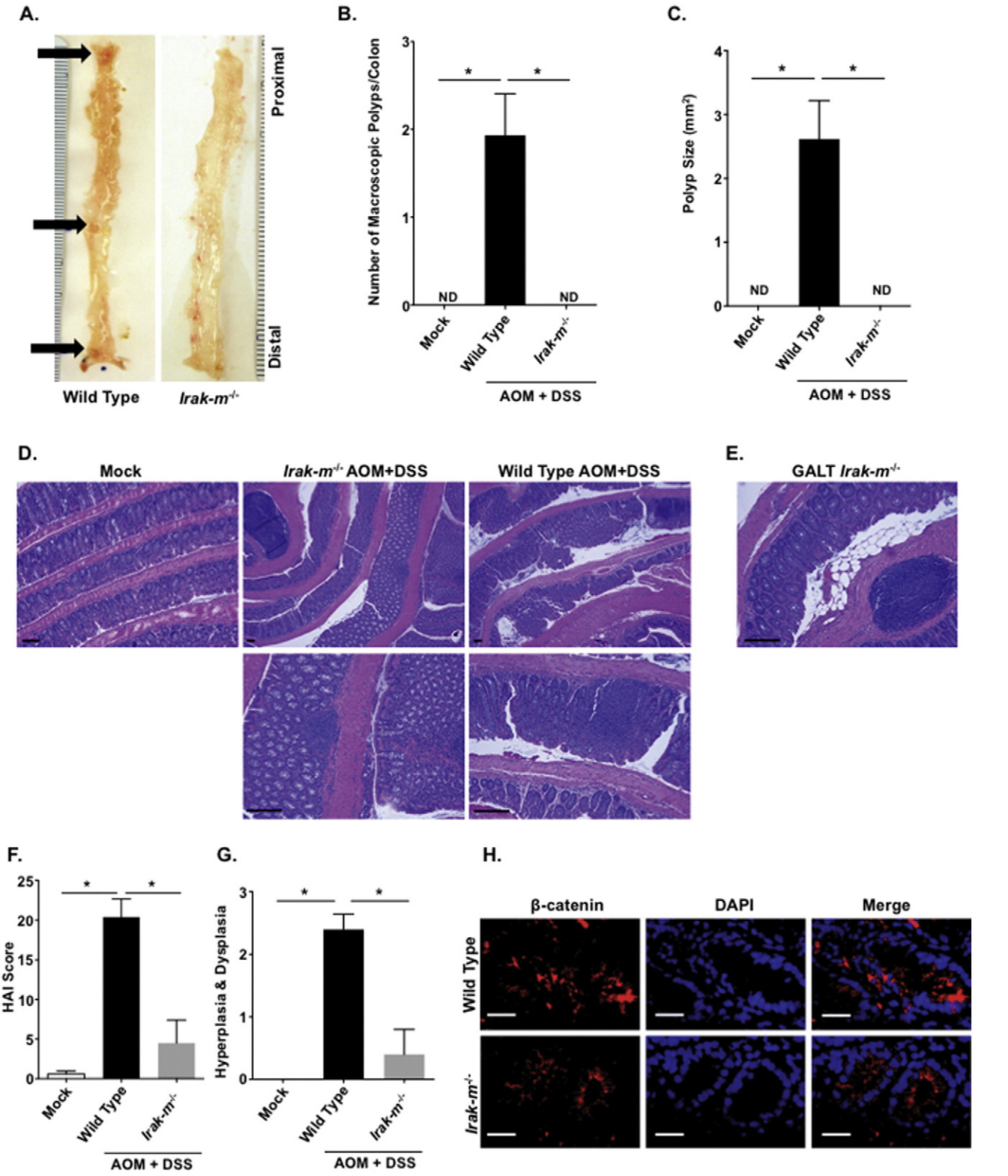

Fig. 5. *Irak-m*$^{-/-}$ mice display attenuated polyp formation in the colitis associated tumorigenesis model. A. Representative image of macroscopic polyp formation in WT and *Irak-m*$^{-/-}$ mice. Black arrows indicate macroscopic polyps in WT mice, with none found in *Irak-m*$^{-/-}$ animals. Scale = mm. B. Average number of macroscopic polyps per colon of WT and *Irak-m*$^{-/-}$ mice following the AOM/DSS model. ND = none detected. C. Average macroscopic polyp size between WT and *Irak-m*$^{-/-}$ mice. D. Representative H&E stained histopathology images of colon sections from WT and *Irak-m*$^{-/-}$ mice following the AOM/DSS model. Scale bars = 100 μm. E. Representative H&E staining of Gut Associated Lymphoid Tissue (GALT) from the colon of *Irak-m*$^{-/-}$ mice following the AOM/DSS model. Areas of expanded GALT were detected in the *Irak-m*$^{-/-}$ mice irrespective of exposure to AOM/DSS. Scale bar = 100 μm F. *Irak-m*$^{-/-}$ mice demonstrated a significant attenuation in histopathological features associated with the AOM/DSS model, as indicated by the histopathological activity index (HAI) score. G. Histopathology assessments also revealed that *Irak-m*$^{-/-}$ mice had significantly attenuated development of hyperplasia and dysplasia compared to the WT animals. H. Representative images of immunofluorescence staining of the colon sections from WT and *Irak-m*$^{-/-}$ mice following the AOM/DSS treatment. The tissue sections were fixed and stained with anti–β-catenin (red) and DAPI (blue). Scale bars = 30 μm. Data are represented as mean ± SEM. *$p < 0.05$; $p < 0.05$ by 1 way ANOVA, Newman-Keuls post-test. Mock WT, $n = 5$ (not shown); mock *Irak-m*$^{-/-}$, $n = 5$ (not shown); AOM + mock WT, $n = 5$; AOM + mock *Irak-m*$^{-/-}$, $n = 5$ (not shown); AOM + DSS WT, $n = 18$; AOM + DSS *Irak-m*$^{-/-}$, $n = 5$. Data are representative of 3 independent studies.

with the combined effects of Wnt and TLR activation (Kesselring et al., 2016). The increase in IRAK-M expression, as well as the expression of other genes that encode negative regulators of PRRs, is likely an attempt to reign in overzealous inflammation and maintain some level of immune system homeostasis during IBD and CRC.

The *Irak-m*$^{-/-}$ mouse model has been an essential tool to determine the negative regulatory mechanisms underlying TLR signaling. *Irak-m*$^{-/-}$ mice have proven to be more sensitive to TLR stimulation and display impaired endotoxin tolerance, likely due to the hyper-activation of NF-κB signaling (Kobayashi et al., 2002). In addition to negatively regulating canonical NF-κB signaling, IRAK-M inhibits the non-canonical NF-κB cascade, in part, through modulating the degradation of NF-κB inducing kinase (NIK) (Su et al., 2009). In prior tumor injection models, loss of *Irak-m*$^{-/-}$ has been shown to result in enhanced innate immune responses and the attenuation of tumor growth (Xie et al., 2007; Standiford et al., 2011). These studies were based on tumor injection models with *Irak-m*$^{-/-}$ mice. However, the overall conclusions of each study are consistent with the observations reported here. In both prior studies, the *Irak-m*$^{-/-}$ animals demonstrated significant resistance to tumor growth and pathogenesis following inoculation. Mechanistically, the attenuation of tumorigenesis was associated with increased activation and proliferation of B cells and T cells, specifically CD4 + and CD8 + T cells (Xie et al., 2007). Our group has previously shown that *Irak-m*$^{-/-}$ macrophages display enhanced uptake of acLDL, as well as increased percentages of macrophages that uptake apoptotic thymocytes (Xie et al., 2007). Reports have demonstrated IL-10R signaling plays a dramatic role in macrophage function (Shouval et al., 2014); additionally, IL-10 is produced from macrophages following the uptake of apoptotic cells (Chung et al., 2007; Zhang et al., 2010). Therefore, though we have not explicitly tested, we speculate that increased phagocytosis of apoptotic cells by *Irak-m* mutant macrophages results in increased IL-10 leading towards a tolerant, and potentially protective phenotype.

Our findings in the experimental colitis and colitis associated tumorigenesis models were initially surprising, as *Irak-m*$^{-/-}$ mice appear to have increased inflammation. However, upon further investigation we discovered that the inflammation is actually highly compartmentalized and isolated to regions of enhanced GALT, with little damage or effect to the epithelial cell barrier. As we detail in the current manuscript, we believe that these expanded areas of GALT are actually beneficial to these mice and function to improve the efficiency of the immune response to translocating microbes from the GI lumen. This is further supported as (Kesselring et al., 2016) described increased GI epithelial barrier permeability in *Irak-m*$^{-/-}$ mice using FITC labeled dextran.

IRAK-M modulation of experimental colitis and colitis associated tumorigenesis has been previously evaluated in *Irak-m*$^{-/-}$ mice (Berglund et al., 2010; Biswas et al., 2011; Klimesova et al., 2013). In the initial study that evaluated IRAK-M function during DSS-induced colitis, *Irak-m*$^{-/-}$ mice were treated with 3% DSS for 5 days and allowed 2 days to recover prior to harvest (Berglund et al., 2010). In this model, *Irak-m*$^{-/-}$ mice were found to be sensitive to DSS and presented with significantly increased clinical and histopathological features associated with disease progression (Berglund et al., 2010). This study also found elevated cytokine, chemokine, and T-cell transcription factor mRNA expression in *Irak-m*$^{-/-}$ colon tissue and increased systemic IL-6 and TNF levels in the plasma following DSS administration (Berglund et al., 2010). Subsequent studies by a different group utilizing the AOM + DSS colitis associated tumorigenesis model in both conventional and germfree conditions also reported increased sensitivity and tumorigenesis in the *Irak-m*$^{-/-}$ mice (Klimesova et al., 2013). Similar to the study by Berglund et al., the *Irak-m*$^{-/-}$ mice were shown to have enhanced pro-inflammatory responses and increased T-cell accumulation in the tumor tissue and local lymph nodes (Klimesova et al., 2013). The mechanism associated with the increased sensitivity was correlated with altered commensal microbe metabolic activity in *Irak-m*$^{-/-}$ mice, suggesting a difference in the microbiome between the WT and *Irak-m*$^{-/-}$ animals (Klimesova et al., 2013). Beyond DSS based models, IRAK-M has also been evaluated in the *Il-10*$^{-/-}$ model of spontaneous colitis (Biswas et al., 2011). Similar to the findings from the DSS models, loss of IRAK-M resulted in increased TLR signaling, resulting in increased inflammation and expression of pro-inflammatory signaling pathways (Biswas et al., 2011). The *Il-10*$^{-/-}$ model is highly dependent on the intestinal commensal flora and subsequent germfree studies evaluating *Irak-m* expression further suggest that *Irak-m*$^{-/-}$ sensitivity in this experimental colitis model is dependent on the composition of the resident GI microbiota (Biswas et al., 2011). The microbiota composition cannot be underestimated for DSS based models as the severity to DSS colitis can drastically change based on the microbiota composition (Hernandez-Chirlaque et al., 2016). We postulate that differences observed between labs utilizing *Irak-m*$^{-/-}$ mice in DSS models could be due to altered microbiome compositions or differing percentages and lots of DSS used among labs.

Though our data provides contradictory evidence compared to the previous findings pertaining to IRAK-M, (Berglund et al., 2010; Biswas et al., 2011; Klimesova et al., 2013) our data is consistent with a more recent study that also showed *Irak-m*$^{-/-}$ mice display reduced tumor burden compared to their WT counterparts in the AOM/DSS model (Kesselring et al., 2016). This was attributed to enhanced epithelial cell barrier function, specifically localized to tumor sites in the GI tract of *Irak-m*$^{-/-}$ mice (Kesselring et al., 2016). This was shown to be associated with reduced activity of the oncogene STAT-3. Our findings described in the current manuscript lend support to this conclusion pertaining to *Irak-m*$^{-/-}$ mice challenged in the AOM/DSS model (Figs. 4 and 5). We further confirm the findings pertaining to decreased Wnt signaling (Kesselring et al., 2016) as demonstrated by the reduced intracellular β-catenin in our study (Fig. 5H). Finally, the analysis of human biopsies from this prior study revealed that human patients with increased IRAK-M expression have worse cancer survival (Kesselring et al., 2016), which corroborates our metadata analysis described (Fig. 1). Collectively, our data pertaining to IRAK-M is complementary to the major findings

Fig. 6. Disruption of the murine *Irak-m* locus results in the formation of an *Irak-m*$^{r\Delta 9-11}$ splice variant. A. Bone marrow derived macrophages (BMDM) from *Irak-m*$^{-/-}$ mice demonstrate increased production of IL-6 following 24 h stimulation with specific PAMPs. Data shown are pooled from 3 separate and independent experiments. $n = 3$ mice per genotype. B. Disruption of the *Irak-m* locus resulted in the loss of Exons 9–11. BMDM from WT and *Irak-m*$^{-/-}$ littermates were un-stimulated or stimulated for 24 h with Pam3CSK4. After 24 h, cells were harvested for RNA and RT-PCR was utilized to amplify *Irak-m* corresponding to exons: 5–8, 9–10, 10–11 and 12, respectively. C. A size difference was detected in the RT-PCR product corresponding to Exons 5–12 between WT and *Irak-m*$^{-/-}$ BMDMs treated for 24 h with Pam3CSK4. The shift of approximately 400 nucleotides in the *Irak-m*$^{-/-}$ BMDMs corresponds to the deleted exons 9, 10 and 11. D. Sequencing of the exon 5–12 RT-PCR product revealed a splice immediately after exon 8 together with exon 12. Normal splicing occurs in the WT BMDM, whereas *Irak-m*$^{-/-}$ BMDM splice around the inserted Neo-cassette after exon 8 and generates a splice variant connecting exon 8 with exon 12. E. (Left) Dual-Luciferase assay of HEK293T cells transfected for 24 h with equal amounts of NF-κB-firefly luciferase reporter plasmid and decreasing amounts of either CMV-WT *Irak-m*-HA plasmid (625 ng–10 ng) or CMV-*Irak-m*$^{r\Delta 9-11}$-HA plasmid (2500 ng–40 ng) from three independent and pooled experiments. Empty Vector is shown as a negative control. β-Galactosidase-HA is shown as a positive control for transfection. A separate β-Galactosidase-HA transfection was treated with 10 ng/mL human IL-1β for 6 h following 18 h of transfection, and serves as a positive control for NF-kB-firefly luciferase activation. All treatment groups received a constant amount of plasmid DNA described in the Supplemental Experimental Methods and are normalized to the Renilla luciferase activity. (Right) Representative western blot of WT IRAK-M and IRAK-M$^{r\Delta 9-11}$ protein expression. Overexpression inserts are HA-tagged at the C-terminus and β-actin is shown as a loading control. The WT IRAK-M expresses readily as seen in the short exposure and migrates at ~68 kDa. The IRAK-M$^{r\Delta 9-11}$ protein is present in the long exposure migrating at ~38 kDa. Data in panel A. is represented as mean ± SEM. $^{*}p < 0.05$ by 1 way ANOVA, Tukey-Kramer post-test. Data in panel E. is represented as mean ± SEM. $^{*}p < 0.001$, $^{\dagger}p < 0.01$ by 1 way ANOVA, Tukey-Kramer post-test. Statistical significance between all treatment groups in E is not shown for simplicity. A minimum of 3 independent experiments were conducted for all assays.

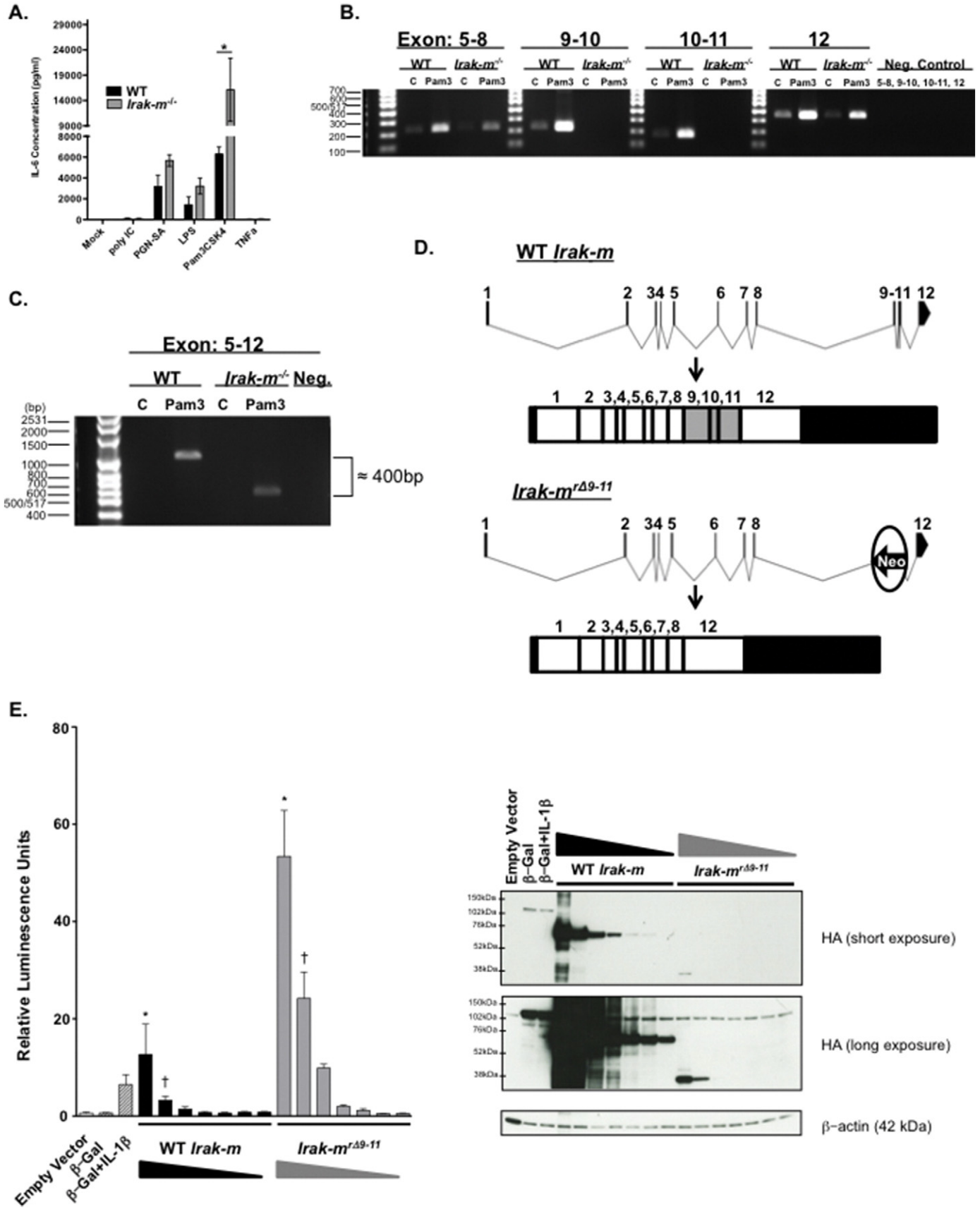
A.
IL-6 Concentration (pg/ml)
WT
Irak-m-/-
Mock
poly IC
PGN-SA
LPS
Pam3CSK4
TNFa
B.
Exon: 5-8
9-10
10-11
12
WT
Irak-m-/-
C
Pam3
Neg. Control
5-8, 9-10, 10-11, 12
C.
Exon: 5-12
WT
Irak-m-/-
Neg.
(bp)
≈ 400bp
D.
WT Irak-m
1 2 34 5 6 7 8 9-11 12
1 2 3,4,5,6,7,8 9,10,11 12
Irak-mrΔ9-11
Neo
1 2 3,4,5,6,7,8 12
E.
Relative Luminescence Units
Empty Vector
β-Gal
β-Gal+IL-1β
WT Irak-m
Irak-mrΔ9-11
HA (short exposure)
HA (long exposure)
β-actin (42 kDa)

by Kesserlring et al. Together, these studies extend the mechanistic insight associated with IRAK-M modulation of IBD and colitis associated tumorigenesis.

IRAK-M functions as a negative regulator of TLR and IL-1R1 signaling by either attenuating the IRAK-1/IRAK-4 phosphorylation event or stabilizing the TLR/MyD88/IRAK-4 complex (Kobayashi et al., 2002). Originally, we sought to better define the mechanisms associated with IRAK-M attenuation of inflammation in the context of experimental colitis and colitis associated tumorigenesis. Through the course of our experiments, our *in vitro* data suggested that BMDMs from *Irak-m*$^{-/-}$ mice displayed an augmented inflammatory response (Fig. 6A**)**, which is consistent with the initial reports characterizing IRAK-M and the *Irak-m*$^{-/-}$ mice (Kobayashi et al., 2002). However, we were intrigued after discovering a protein band pertaining to IRAK-M in BMDMs from the *Irak-m*$^{-/-}$ mice after treating with specific pathogenic ligands (Fig. S1). As previously described in the original manuscript reporting the generation of *Irak-m*$^{-/-}$ mice, exons 9–11 were targeted for deletion by homologous recombination and the insertion of a neo cassette (Kobayashi et al., 2002). Our genotyping confirms the successful targeting of *Irak-m*. However, as we show in our current studies, a splice variant of the *Irak-m* gene is formed following BMDM stimulation in the targeted *Irak-m*$^{-/-}$ animals. The splicing event circumvents the neo cassette and joins exon 8 with exon 12, defined here as *Irak-m*$^{r\Delta 9-11}$. Together, our data suggests that the inclusion of exon 12 in the mRNA effectively stabilizes the transcript. Further functional studies using overexpression systems revealed that this truncation has the potential to robustly activate NF-κB signaling (Fig. 6E). If this splice variant is present in the *Irak-m*$^{-/-}$ mice, then it is possible that the *Irak-m*$^{r\Delta 9-11}$ variant could result in potential phenotypes not characteristic of a true knockout mouse. These could include reduced or hyperactive activity for IRAK-M functioning as either a dominant negative or potentially even a dominant positive.

In conclusion, our data strongly suggests that IRAK-M functions to modulate inflammatory signaling pathways and is critical in maintaining immune system homeostasis in the gut. However, increased IRAK-M is associated with increased disease pathogenesis and increased cancer severity in human patients. Our findings in mice revealed that the immune system in *Irak-m*$^{-/-}$ animals is primed and highly efficient at eliminating microbes translocating from the GI lumen. This increased microbial clearance is associated with reduced experimental colitis and colitis associated tumorigenesis. Together, our data identify IRAK-M as an essential regulator of inflammation and is critical in the maintenance of mucosal immune system homeostasis in health and disease.

Funding Sources

This work was supported by the National Institute of Diabetes and Digestive and Kidney Diseases under awards K01DK092355, R03DK105975, and grant funding through the Virginia-Maryland College of Veterinary Medicine (2013) (I. Allen). The content is solely the responsibility of the authors and does not necessarily represent the official views of the NIH.

Conflicts of Interest

The authors declare no conflict of interest.

Author Contributions

Conceptualization, D.E.R, Y.Z., N.D., C.K.L., K.C., C.C.C., L.L., I.C.A.; Methodology, D.E.R, Y.Z., N.D., C.K.L, K.C., L.L., I.C.A.; Formal Analysis, T.L., L.L., I.C.A.; Investigation, D.E.R., Y.Z., N.D., C.K.L., K.C., C.C.C., D.J.S., I.C.A.; Resources, C.C.C.; D.J.S., R.F.H., L.L., I.C.A.; Writing-Original Draft, D.E.R. and I.C.A.; Supervision, C.C.C., L.L., I.C.A.; Funding Acquisition, L.L. and I.C.A.

Acknowledgements

We kindly thank Bettina Heid for her technical assistance, and Dr. Renata L.S. Goncalves for scientific suggestions and critically reviewing our manuscript. We would like to thank the makers of wormweb.org for the publically available Exon-Intron graphic designer and the makers of Primer3.

Appendix A. Supplementary data

Supplemental Information includes four figures and Supplemental Experimental Procedures. Supplementary data associated with this article can be found in the online version, at http://dx.doi.org/10.1016/j.ebiom.2016.11.039.

References

Allen, I.C., Tekippe, E.M., Woodford, R.M., Uronis, J.M., Holl, E.K., Rogers, A.B., Herfarth, H.H., Jobin, C., Ting, J.P., 2010. The NLRP3 inflammasome functions as a negative regulator of tumorigenesis during colitis-associated cancer. J. Exp. Med. 207, 1045–1056.

Allen, I.C., Wilson, J.E., Schneider, M., Lich, J.D., Roberts, R.A., Arthur, J.C., Woodford, R.M., Davis, B.K., Uronis, J.M., Herfarth, H.H., Jobin, C., Rogers, A.B., Ting, J.P., 2012. NLRP12 suppresses colon inflammation and tumorigenesis through the negative regulation of noncanonical NF-kappaB signaling. Immunity 36, 742–754.

Berglund, M., Melgar, S., Kobayashi, K.S., Flavell, R.A., Hornquist, E.H., Hultgren, O.H., 2010. IL-1 receptor-associated kinase M downregulates DSS-induced colitis. Inflamm. Bowel Dis. 16, 1778–1786.

Biswas, A., Wilmanski, J., Forsman, H., Hrncir, T., Hao, L., Tlaskalova-Hogenova, H., Kobayashi, K.S., 2011. Negative regulation of Toll-like receptor signaling plays an essential role in homeostasis of the intestine. Eur. J. Immunol. 41, 182–194.

Boj, S.F., Hwang, C.I., Baker, L.A., Chio, I.I., Engle, D.D., Corbo, V., Jager, M., Ponz-Sarvise, M., Tiriac, H., Spector, M.S., Gracanin, A., Oni, T., Yu, K.H., Van Boxtel, R., Huch, M., Rivera, K.D., Wilson, J.P., Feigin, M.E., Ohlund, D., Handly-Santana, A., Ardito-Abraham, C.M., Ludwig, M., Elyada, E., Alagesan, B., Biffi, G., Yordanov, G.N., Delcuze, B., Creighton, B., Wright, K., Park, Y., Morsink, F.H., Molenaar, I.Q., Borel Rinkes, I.H., Cuppen, E., Hao, Y., Jin, Y., Nijman, I.J., Iacobuzio-Donahue, C., Leach, S.D., Pappin, D.J., Hammell, M., Klimstra, D.S., Basturk, O., Hruban, R.H., Offerhaus, G.J., Vries, R.G., Clevers, H., Tuveson, D.A., 2015. Organoid models of human and mouse ductal pancreatic cancer. Cell 160, 324–338.

Chung, E.Y., Liu, J., Homma, Y., Zhang, Y., Brendolan, A., Saggese, M., Han, J., Silverstein, R., Selleri, L., Ma, X., 2007. Interleukin-10 expression in macrophages during phagocytosis of apoptotic cells is mediated by homeodomain proteins Pbx1 and Prep-1. Immunity 27, 952–964.

Cook, D.N., Pisetsky, D.S., Schwartz, D.A., 2004. Toll-like receptors in the pathogenesis of human disease. Nat. Immunol. 5, 975–979.

Fernandes, P., Macsharry, J., Darby, T., Fanning, A., Shanahan, F., Houston, A., Brint, E., 2016. Differential expression of key regulators of Toll-like receptors in ulcerative colitis and Crohn's disease: a role for Tollip and peroxisome proliferator-activated receptor gamma? Clin. Exp. Immunol. 183, 358–368.

Greten, F.R., Eckmann, L., Greten, T.F., Park, J.M., Li, Z.W., Egan, L.J., Kagnoff, M.F., Karin, M., 2004. IKKbeta links inflammation and tumorigenesis in a mouse model of colitis-associated cancer. Cell 118, 285–296.

Gunaltay, S., Nyhlin, N., Kumawat, A.K., Tysk, C., Bohr, J., Hultgren, O., Hultgren Hornquist, E., 2014. Differential expression of interleukin-1/Toll-like receptor signaling regulators in microscopic and ulcerative colitis. World J. Gastroenterol. 20, 12249–12259.

Hammer, G.E., Turer, E.E., Taylor, K.E., Fang, C.J., Advincula, R., Oshima, S., Barrera, J., Huang, E.J., Hou, B., Malynn, B.A., Reizis, B., Defranco, A., Criswell, L.A., Nakamura, M.C., Ma, A., 2011. Expression of A20 by dendritic cells preserves immune homeostasis and prevents colitis and spondyloarthritis. Nat. Immunol. 12, 1184–1193.

Hernandez-Chirlaque, C., Aranda, C.J., Ocon, B., Capitan-Canadas, F., Ortega-Gonzalez, M., Carrero, J.J., Suarez, M.D., Zarzuelo, A., Sanchez De Medina, F., Martinez-Augustin, O., 2016. Germ-free and antibiotic-treated mice are highly susceptible to epithelial injury in DSS colitis. J. Crohns Colitis 10, 1324–1335.

Hoebe, K., Du, X., Georgel, P., Janssen, E., Tabeta, K., Kim, S.O., Goode, J., Lin, P., Mann, N., Mudd, S., Crozat, K., Sovath, S., Han, J., Beutler, B., 2003. Identification of Lps2 as a key transducer of MyD88-independent TIR signalling. Nature 424, 743–748.

Jiang, Z., Georgel, P., Li, C., Choe, J., Crozat, K., Rutschmann, S., Du, X., Bigby, T., Mudd, S., Sovath, S., Wilson, I.A., Olson, A., Beutler, B., 2006. Details of Toll-like receptor:adapter interaction revealed by germ-line mutagenesis. Proc. Natl. Acad. Sci. U. S. A. 103, 10961–10966.

Karlen, P., Lofberg, R., Brostrom, O., Leijonmarck, C.E., Hellers, G., Persson, P.G., 1999. Increased risk of cancer in ulcerative colitis: a population-based cohort study. Am. J. Gastroenterol. 94, 1047–1052.

Kawai, T., Akira, S., 2011. Toll-like receptors and their crosstalk with other innate receptors in infection and immunity. Immunity 34, 637–650.

Kawai, T., Adachi, O., Ogawa, T., Takeda, K., Akira, S., 1999. Unresponsiveness of MyD88-deficient mice to endotoxin. Immunity 11, 115–122.

Kawai, T., Takeuchi, O., Fujita, T., Inoue, J., Muhlradt, P.F., Sato, S., Hoshino, K., Akira, S., 2001. Lipopolysaccharide stimulates the MyD88-independent pathway and results in activation of IFN-regulatory factor 3 and the expression of a subset of lipopolysaccharide-inducible genes. J. Immunol. 167, 5887–5894.

Kesselring, R., Glaesner, J., Hiergeist, A., Naschberger, E., Neumann, H., Brunner, S.M., Wege, A.K., Seebauer, C., Kohl, G., Merkl, S., Croner, R.S., Hackl, C., Sturzl, M., Neurath, M.F., Gessner, A., Schlitt, H.J., Geissler, E.K., Fichtner-Feigl, S., 2016. IRAK-M expression in tumor cells supports colorectal cancer progression through reduction of antimicrobial defense and stabilization of STAT3. Cancer Cell 29, 684–696.

Klimesova, K., Kverka, M., Zakostelska, Z., Hudcovic, T., Hrncir, T., Stepankova, R., Rossmann, P., Ridl, J., Kostovcik, M., Mrazek, J., Kopecny, J., Kobayashi, K.S., Tlaskalova-Hogenova, H., 2013. Altered gut microbiota promotes colitis-associated cancer in IL-1 receptor-associated kinase M-deficient mice. Inflamm. Bowel Dis. 19, 1266–1277.

Kobayashi, K., Hernandez, L.D., Galan, J.E., Janeway Jr., C.A., Medzhitov, R., Flavell, R.A., 2002. IRAK-M is a negative regulator of Toll-like receptor signaling. Cell 110, 191–202.

Kupershmidt, I., Su, Q.J., Grewal, A., Sundaresh, S., Halperin, I., Flynn, J., Shekar, M., Wang, H., Park, J., Cui, W., Wall, G.D., Wisotzkey, R., Alag, S., Akhtari, S., Ronaghi, M., 2010. Ontology-based meta-analysis of global collections of high-throughput public data. PLoS One 5.

Li, S., Strelow, A., Fontana, E.J., Wesche, H., 2002. IRAK-4: a novel member of the IRAK family with the properties of an IRAK-kinase. Proc. Natl. Acad. Sci. U. S. A. 99, 5567–5572.

Medzhitov, R., Janeway Jr., C.A., 1997. Innate immunity: the virtues of a nonclonal system of recognition. Cell 91, 295–298.

Mukherjee, S., Biswas, T., 2014. Activation of TOLLIP by porin prevents TLR2-associated IFN-gamma and TNF-alpha-induced apoptosis of intestinal epithelial cells. Cell. Signal. 26, 2674–2682.

Muzio, M., Ni, J., Feng, P., Dixit, V.M., 1997. IRAK (Pelle) family member IRAK-2 and MyD88 as proximal mediators of IL-1 signaling. Science 278, 1612–1615.

Neufert, C., Becker, C., Neurath, M.F., 2007. An inducible mouse model of colon carcinogenesis for the analysis of sporadic and inflammation-driven tumor progression. Nat. Protoc. 2, 1998–2004.

Okayasu, I., Hatakeyama, S., Yamada, M., Ohkusa, T., Inagaki, Y., Nakaya, R., 1990. A novel method in the induction of reliable experimental acute and chronic ulcerative colitis in mice. Gastroenterology 98, 694–702.

Saleh, M., Elson, C.O., 2011. Experimental inflammatory bowel disease: insights into the host-microbiota dialog. Immunity 34, 293–302.

Schneider, M., 2013. Dextran sodium sulfate-induced murine inflammatory colitis model. Methods Mol. Biol. 1031, 189–195.

Shouval, D.S., Biswas, A., Goettel, J.A., Mccann, K., Conaway, E., Redhu, N.S., Mascanfroni, I.D., Al Adham, Z., Lavoie, S., Ibourk, M., Nguyen, D.D., Samsom, J.N., Escher, J.C., Somech, R., Weiss, B., Beier, R., Conklin, L.S., Ebens, C.L., Santos, F.G., Ferreira, A.R., Sherlock, M., Bhan, A.K., Muller, W., Mora, J.R., Quintana, F.J., Klein, C., Muise, A.M., Horwitz, B.H., Snapper, S.B., 2014. Interleukin-10 receptor signaling in innate immune cells regulates mucosal immune tolerance and anti-inflammatory macrophage function. Immunity 40, 706–719.

Singh, K., Poteryakhina, A., Zheltukhin, A., Bhatelia, K., Prajapati, P., Sripada, L., Tomar, D., Singh, R., Singh, A.K., Chumakov, P.M., Singh, R., 2015. NLRX1 acts as tumor suppressor by regulating TNF-alpha induced apoptosis and metabolism in cancer cells. Biochim. Biophys. Acta 1853, 1073–1086.

Soares, F., Tattoli, I., Rahman, M.A., Robertson, S.J., Belcheva, A., Liu, D., Streutker, C., Winer, S., Winer, D.A., Martin, A., Philpott, D.J., Arnoult, D., Girardin, S.E., 2014. The mitochondrial protein NLRX1 controls the balance between extrinsic and intrinsic apoptosis. J. Biol. Chem. 289, 19317–19330.

Standiford, T.J., Kuick, R., Bhan, U., Chen, J., Newstead, M., Keshamouni, V.G., 2011. TGF-beta-induced IRAK-M expression in tumor-associated macrophages regulates lung tumor growth. Oncogene 30, 2475–2484.

Su, J., Zhang, T., Tyson, J., Li, L., 2009. The interleukin-1 receptor-associated kinase M selectively inhibits the alternative, instead of the classical NFkappaB pathway. J. Innate Immun. 1, 164–174.

Takeuchi, O., Takeda, K., Hoshino, K., Adachi, O., Ogawa, T., Akira, S., 2000. Cellular responses to bacterial cell wall components are mediated through MyD88-dependent signaling cascades. Int. Immunol. 12, 113–117.

Vereecke, L., Vieira-Silva, S., Billiet, T., Van Es, J.H., Mc Guire, C., Slowicka, K., Sze, M., Van Den Born, M., De Hertogh, G., Clevers, H., Raes, J., Rutgeerts, P., Vermeire, S., Beyaert, R., Van Loo, G., 2014. A20 controls intestinal homeostasis through cell-specific activities. Nat. Commun. 5, 5103.

Wesche, H., Henzel, W.J., Shillinglaw, W., Li, S., Cao, Z., 1997. MyD88: an adapter that recruits IRAK to the IL-1 receptor complex. Immunity 7, 837–847.

Wesche, H., Gao, X., Li, X., Kirschning, C.J., Stark, G.R., Cao, Z., 1999. IRAK-M is a novel member of the Pelle/interleukin-1 receptor-associated kinase (IRAK) family. J. Biol. Chem. 274, 19403–19410.

Williams, T.M., Leeth, R.A., Rothschild, D.E., Coutermarsh-Ott, S.L., Mcdaniel, D.K., Simmons, A.E., Heid, B., Cecere, T.E., Allen, I.C., 2015a. The NLRP1 inflammasome attenuates colitis and colitis-associated tumorigenesis. J. Immunol. 194, 3369–3380.

Williams, T.M., Leeth, R.A., Rothschild, D.E., Mcdaniel, D.K., Coutermarsh-Ott, S.L., Simmons, A.E., Kable, K.H., Heid, B., Allen, I.C., 2015b. Caspase-11 attenuates gastrointestinal inflammation and experimental colitis pathogenesis. Am. J. Physiol. Gastrointest. Liver Physiol. 308, G139–G150.

Xie, Q., Gan, L., Wang, J., Wilson, I., Li, L., 2007. Loss of the innate immunity negative regulator IRAK-M leads to enhanced host immune defense against tumor growth. Mol. Immunol. 44, 3453–3461.

Yamamoto, M., Sato, S., Hemmi, H., Hoshino, K., Kaisho, T., Sanjo, H., Takeuchi, O., Sugiyama, M., Okabe, M., Takeda, K., Akira, S., 2003. Role of adaptor TRIF in the MyD88-independent toll-like receptor signaling pathway. Science 301, 640–643.

Zaki, M.H., Vogel, P., Malireddi, R.K., Body-Malapel, M., Anand, P.K., Bertin, J., Green, D.R., Lamkanfi, M., Kanneganti, T.D., 2011. The NOD-like receptor NLRP12 attenuates colon inflammation and tumorigenesis. Cancer Cell 20, 649–660.

Zhang, Y., Kim, H.J., Yamamoto, S., Kang, X., Ma, X., 2010. Regulation of interleukin-10 gene expression in macrophages engulfing apoptotic cells. J. Interf. Cytokine Res. 30, 113–122.